NRL 2563

29 May 1945

NAVAL RESEARCH LABORATORY
WASHINGTON 20, D. C.

TRANSMISSION, REFLECTION, AND GUIDING OF AN EXPONENTIAL PULSE BY A STEEL PLATE IN WATER. 1. THEORY

by
M. F. M. Osborne, Physicist
and
S. D. Hart, CSp (X) USNR

Acc. No. 705

Sound Division - Special Research
Report No. S-2563

Approved by
P. N. Arnold,
Head, Special Research Section

Dr. H. C. Hayes
Superintendent, Sound Division

A. H. Van Keuren, Rear Admiral USN
Director, Naval Research Laboratory

Title Page
Abstract
Table of Contents
Text - - - 36
Tables - - 0
Plates - - 6

ABSTRACT

In this report the problem of the interaction of an underwater explosion wave with a steel plate is discussed. Particular attention is given to those aspects of the problem in which the plate can be considered as a two-dimensional wave guide. The phase velocities of the more important modes of the plate are evaluated as functions of frequency. They are used to derive the properties of the precursor, an oscillation which precedes the explosion wave as it travels along the plate. The results of the theory are compared briefly with experiment. A more detailed discussion of the experiments will be given in a second report.

The methods used in this report are also applicable to the evaluation of the phase velocities of the modes of an electromagnetic wave guide. The propagation of a transient, such as an explosion wave, down a wave guide presents the interesting mathematical problem of the evaluation of a contour integral of a function of a complex variable defined implicitly. No rigorous solution for this problem as yet exists.

TABLE OF CONTENTS

PLATES

I. INTRODUCTION

1. In a second report under the same title an account will be given of experiments measuring the pressure caused by the explosion of a No. 8 Dupont blasting cap in the neighborhood of a steel disc in water; in this report is presented a theoretical study of the same problem. This study is primarily intended to give a theoretical explanation of the "precursor". This is a characteristic oscillation which, for oblique angles of incidence, preceded the explosion wave as it traversed the diameter of the disc, as is shown in Plate 8.

2. All the experimental phenomena observed, except the existence and properties of the precursor, can be explained on the basis of theory already developed. In this report the problem of the action of an exponential transient (the explosion wave) on a steel plate will be discussed, with special attention to those aspects of the problem concerned with the precursor. Essentially, the problem to be solved is that of the two-dimensional wave guide formed by an elastic plate in water.

II. STATEMENT OF THE PROBLEM

3. The problem will first be stated in complete generality, and then be simplified and approximated until it becomes tractable. It must be remembered that a complete solution is not desired, but only those properties of the solution which can be compared with experiments. In particular it is desired to know the pressure as a function of time for a specified position near the disc before the arrival of the main shock, i.e. the properties of the precursor. By "properties" is meant the approximate period of the pressure fluctuations, when they appear and how long they last.

4. Let the displacement of the medium be given by

$$\vec{r}_s = \text{grad}\ \varphi_s + \text{curl}\ \vec{\psi}_s$$
$$\vec{r}_w = \text{grad}\ \varphi_w \qquad (1)$$

where the subscripts w,s, refer to the water and steel. It is required to find functions φ and $\vec{\psi}$ satisfying the wave equations

$$(\nabla^2 - \frac{1}{c_r^2}\frac{\partial^2}{\partial t^2})\varphi_s = 0$$

$$(\nabla^2 - \frac{1}{c_d^2}\frac{\partial^2}{\partial t^2})\vec{\psi}_s = 0$$

$$(\nabla^2 - \frac{1}{c_w^2}\frac{\partial^2}{\partial t^2})\varphi_w = 0 \qquad (2)$$

subject to the boundary conditions:

r_n continuous on the water-steel boundary,
p_n continuous on the water-steel boundary,
$p_t = 0$ in water and on the water-steel boundary.
r_n is the normal displacement in the medium, and
p_n and p_t are the normal and tangential stresses.

The notation follows References 1 and 2.

5. The initial conditions are set by the requirement that the incident wave be a diverging wave of exponential form. If time is measured from the instant that the explosion wave just touches the plate, then at $t = 0$,

$$p_n = \frac{e^{r/c_w \tau}}{r} \qquad r < R$$

$$= 0 \qquad r > R \qquad (3)$$

where r is the distance coordinate measured from the explosion source, and R the distance to the nearest point of the plate. τ is the "time constant" of the exponential explosion wave, and c_w the velocity of sound in water.

6. This problem is first simplified by replacing it by a two-dimensional one, since in the experiments the distance to the explosion source (11 feet 6 inches) was large compared to the radius of the disc (1 foot). The disc is taken as a semi-infinite slab, the incident wave is now plane instead of spherical, and the motion takes place in two dimensions only (Sketch 1).

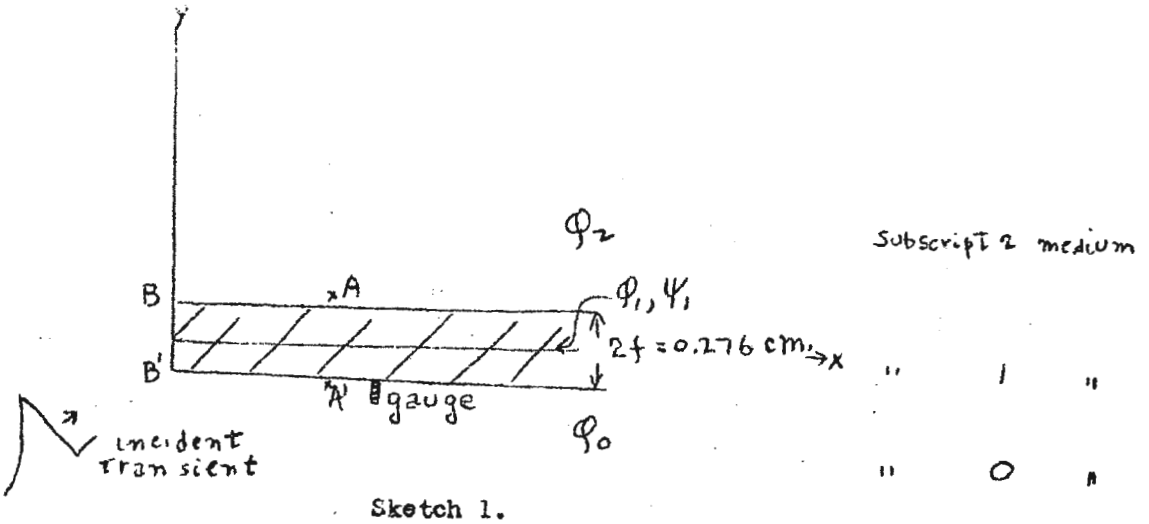

Sketch 1.

This approximation can be expected to be best up to a time shortly after the arrival of the explosion wave in the water, and to describe disturbances whose dimensions are small compared to the radius of the disc.

7. The problem can be still further simplified. Since the observations refer to conditions close to the plate, i.e., at points such as A and A', one would like to determine φ_W at these points as functions of time, and at various distances from the edge BB'. It is known from the observations that the diffracted wave is small. The problem of determining φ_W at A or A' is therefore divided into two parts: (1) a part due to the transmission of the wave through the plate, or its reflection from the plate, considered as infinite, and (2) a part arising from the forces or displacements obtaining initially at the edge of the plate (BB') due to the explosion wave.

8. The first problem is then one of the reflection or transmission of a plane wave transient at an infinite plane plate. The second problem is that of the plate considered as a two-dimensional "wave guide", with specified initial conditions. Both of these problems can be solved by first obtaining the solution for steady-state sinusoidal time dependence, and then superposing by integration solutions for different frequencies in order to represent the incident transient, or initial conditions.

9. The first problem, the reflection and transmission of sinusoidal waves at an infinite plate, has been solved by Reissner (Ref. 3). He assumes an incident wave of amplitude unity, and of arbitrary frequency and angle of incidence θ. In order to satisfy the six boundary conditions, three on each side of the plate, and the conditions that the amplitudes of all the progressive waves set up be independent of the coordinate along the plate (x) and time, just six additional waves with amplitudes different from zero must be found. There are one reflected wave, four waves inside the plate (one dilation, one rotation, in each direction $\pm$ y), and one transmitted wave. There are therefore seven wave amplitudes (one specified as unity), and six boundary conditions. These boundary conditions give

a set of six inhomogeneous equations on the six unknown amplitudes, which are thus completely determined. In analogy with the corresponding electromagnetic problem of reflection from a lamina, this may be called the inhomogeneous problem of waves in an elastic plate in water.

10. The homogeneous problem is the one in which the plate is considered a two-dimensional wave guide. Here there are four waves inside the plate, and only two in the water, one on each side of the plate. With six waves in all, the six boundary conditions give a set of six homogeneous linear equations to be satisfied by the wave amplitudes. There is therefore no solution unless the determinant of the coefficients of the amplitudes vanishes. This determinant determines the normal modes, or a discrete set of space distribution constants, for any specified frequency. Only one of the six amplitudes can be specified arbitrarily; the rest are determined.

III. THE INHOMOGENEOUS CASE

11. Reissner's solution to the inhomogeneous problem can be used to determine the shape of the transient reflected or transmitted through the plate as follows. He obtains the amplitudes $A_{r\theta}(\omega)$ and $A_{r\theta}(\omega)$ of the transmitted and reflected waves when a sinusoid of amplitude unity, circular frequency ω, at angle θ is incident on the plate. If a plane wave transient at an angle of incidence θ has the form or profile (ignoring the dependence on position)

$$f_\theta(t) = e^{-t/\tau} \quad t > 0$$
$$= 0 \quad t < 0 \tag{4}$$

then the reflected wave is

$$R(t) = \frac{1}{\sqrt{2\pi}} \int_{-\infty}^{+\infty} g_\theta(\omega)\, A_{r\theta}(\omega)\, e^{-i\omega\tau}\, d\omega \tag{5}$$

and the transmitted wave is

$$T(t) = \frac{1}{\sqrt{2\pi}} \int_{-\infty}^{+\infty} g_\theta(\omega)\, A_{t\theta}(\omega)\, e^{-i\omega t}\, d\omega \tag{6}$$

where $g_\theta(\omega)$ is the Fourier transform of $f_\theta(t)$.

$$g_\theta(\omega) = \frac{1}{\sqrt{2\pi}} \int_{-\infty}^{+\infty} f_\theta(t)\, e^{i\omega t}\, d\omega \tag{7}$$

12. The effect of the functions $A_{t\theta}(\omega)$, $A_{r\theta}(\omega)$ in cutting out parts of the Fourier spectrum is as follows. If $A_{t\theta}(\omega)$ is small (compared to unity) at high frequencies, and of order unity at low frequencies, the shock front of the transmitted exponential wave will be rounded off and the height of the peak diminished. If $A_{r\theta}(\omega)$ is of order unity at high frequencies and small at low frequencies, the reflected wave preserves its steep shock front, but falls off more rapidly than the incident wave and may even become negative. These effects are illustrated qualitatively in Sketch 2, and in Plate 8, Nos. 2, 1. Detailed data and discussion will be given in the second report (II) on this work.

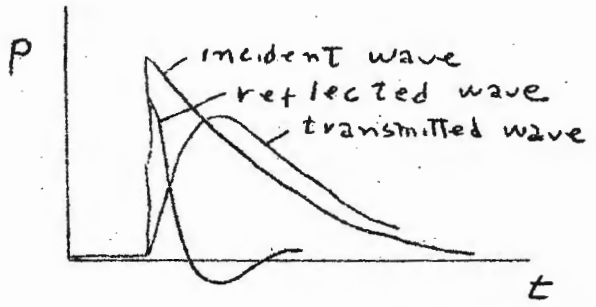

Sketch 2.

IV. THE HOMOGENEOUS CASE

13. The homogeneous, or wave-guide problem will form the main subject of this report, and will be used to derive some properties of the precursor. It will therefore be stated more completely than the inhomogeneous case discussed above. The notation and method will follow that of Lamb in Ref. 2, where the problem of a plate in a vacuum is solved. Some familiarity with Lamb's paper must be assumed, as his solution was used as a basis for solving the present problem. The two are closely related.

14. The steady-state wave-guide problem may be stated as follows. Find the functions φ and ψ such that (See Sketch 1):

In the water,

$$\nabla^2 \varphi_0 - \frac{1}{c_w^2} \frac{\partial^2 \varphi_0}{\partial t^2} = 0$$

$$\nabla^2 \varphi_2 - \frac{1}{c_w^2} \frac{\partial^2 \varphi_2}{\partial t^2} = 0 \qquad (8)$$

In the plate,

$$\nabla^2 \varphi_1 - \frac{1}{c_d^2} \frac{\partial^2 \varphi_1}{\partial t^2} = 0$$
$$\nabla^2 \psi_1 - \frac{1}{c_r^2} \frac{\partial^2 \psi_1}{\partial t^2} = 0 \qquad (9)$$

Displacement in x,

$$u = \frac{\partial \varphi_1}{\partial x} + \frac{\partial \psi_1}{\partial y}$$

Displacement in y,

$$v = \frac{\partial \varphi_1}{\partial y} - \frac{\partial \psi_1}{\partial x} \qquad (10)$$

in the plate.

In the water,

$$u = \frac{\partial \varphi_{0 \text{ or } 2}}{\partial x}, \quad v = \frac{\partial \varphi_{0 \text{ or } 2}}{\partial y}$$

Velocity of dilational waves in the plate,

$$c_d = \sqrt{\frac{\lambda_s + 2\mu_s}{\rho_s}} = 0.57 \cdot 10^6 \text{ cm/sec}$$

Velocity of rotational waves in the plate, (11)

$$c_r = \sqrt{\frac{\mu_s}{\rho_s}} = 0.33 \cdot 10^6 \text{ cm/sec}$$

Velocity of dilational (sound) waves in the water,

$$c_w = \sqrt{\frac{\lambda_w}{\rho_w}} = 0.15 \cdot 10^6 \text{ cm/sec}$$

λ and μ are Lamé's constants, and Poisson's assumption that $\lambda_s = \mu_s$ is made for the plate. $\rho_w = 1.0$, $\rho_s = 7.6$ gm/cm3. The half-thickness, f, of the plate is 0.138 cm.

15. Boundary conditions at $y = \pm f$.

(1) P_{yy} is continuous at $y = \pm f$. (12)

$(P_{yy})_1 = (P_{yy})_0$ at $y = -f$.

$(P_{yy})_1 = (P_{yy})_2$ at $y = +f$.

$$P_{yy} = \lambda \left(\frac{\partial u}{\partial x} + \frac{\partial v}{\partial y} \right) + 2\mu \frac{\partial v}{\partial y}$$

(2) P_{xy} vanishes at $y = \pm f$

$$(P_{xy})_1 = 0 \text{ at } y = \pm f$$
$$P_{xy} = \mu\left(\frac{\partial v}{\partial x} + \frac{\partial u}{\partial y}\right) \qquad (13)$$

(3) v is continuous at $y = \pm f$

$$v_1 = v_0 \text{ at } y = -f$$
$$v_1 = v_2 \text{ at } y = +f \qquad (14)$$

16. The solution is required to be of the form $f(x,y)e^{i\omega t}$ with ω the same in plate and water. The variables are assumed separable, the separation constants in y being $-\eta_1^2, -\alpha_1^2, -\beta_1^2, -\eta_1^2$ for $\varphi_0, \varphi_1, \psi_1, \varphi_2$ respectively. The separation constant $-\xi^2$ for x must be the same for all φ's and ψ, for the desired wave amplitudes to be independent of x. This same requirement also specifies only one sign for ξ, either + or -, i.e., that waves travel in only one direction in x along the plate. Then it can be easily verified that the solutions can be written in the form (all progressive waves),

$$\varphi_0 = A_0 e^{i(\omega t + \xi x + \eta_1 y)}$$
$$\varphi_1 = A_d' e^{i(\omega t + \xi x + \alpha_1 y)} + B_d' e^{i(\omega t + \xi x - \alpha_1 y)}$$
$$\psi_1 = A_r' e^{i(\omega t + \xi x + \beta_1 y)} + B_r' e^{i(\omega t + \xi x - \beta_1 y)} \qquad (15)$$
$$\varphi_2 = A_2 e^{i(\omega t + \xi x - \eta_1 y)}$$

The separation constants are related to ω as follows:

$$\xi^2 + \eta_1^2 = \frac{\omega^2}{c_w^2}, \quad \xi^2 + \alpha_1^2 = \frac{\omega^2}{c_d^2}, \quad \xi^2 + \beta_1^2 = \frac{\omega^2}{c_r^2} \qquad (16)$$

17. In this form only the indicated choices of sign are allowed for $i\eta_1$, to insure either an outgoing wave from the plate for $i\eta_1$ imaginary, or finiteness at infinity, for $i\eta_1$ real.

18. Equations (15) can be rewritten, for purposes of convenience, in the following form (standing waves in y only),

$$\varphi_0 = A_0 e^{+\eta y} \; e^{i(\omega T + \xi x)}$$

$$\varphi_1 = (A_d \cosh \alpha y + B_d \sinh \alpha y) e^{i(\omega T + \xi x)} \qquad (17)$$

$$\psi_1 = (A_r \cosh \beta y + B_r \sinh \beta y) e^{i(\omega T + \xi x)}$$

$$\varphi_2 = A_2 e^{-\eta y} \; e^{i(\omega T + \xi x)}$$

where

$$\xi^2 - \eta^2 = \frac{\omega^2}{c_w^2} \; , \quad \xi^2 - \alpha^2 = \frac{\omega^2}{c_d^2} \; , \quad \xi^2 - \beta^2 = \frac{\omega^2}{c_r^2} \qquad (18)$$

19. If the equations (17) are substituted into the boundary conditions (12), (13), (14), the six equations (19) (Page 12) are obtained. The common factor $e^{i(\omega T + \xi x)}$ has been cancelled from them all, and the common amplitude factor of each column is indicated at the top.

20. For a solution for the A's and B's to exist, the determinant of their coefficients must vanish. This determinant, for a given ω , determines the allowed values of ξ , and hence of α, β, η . There is in general an infinite set of discrete values for ξ, α, β, η for any given ω . They may be real or complex.

21. The determinant of the coefficients in (19) can be rearranged as is indicated in (20) (Page 13).

22. This form is more suitable for determining the various roots $\xi_i, \alpha_i, \beta_i, \eta_i$ for a given ω . In this form it is evident that either the upper or lower diagonal minor can be set equal to zero, as a condition that the entire determinant shall vanish.

23. This division of the sixth order determinant into the product of two third order determinants has a simple physical interpretation. It is possible to satisfy all six boundary conditions using four waves, with only three different amplitudes. One can use (21)

A_0	A_d	A_r	B_d	B_r	A_2	
0	$\alpha \sinh\alpha f$	$-i\xi \cosh\beta f$	$+\alpha \cosh\alpha f$	$-i\xi \sinh\beta f$	$+\eta e^{-\eta f}$	$=0$
$-\eta e^{-\eta f}$	$-\alpha \sinh\alpha f$	$-i\xi \cosh\beta f$	$+\alpha \cosh\alpha f$	$+i\xi \sinh\beta f$	0	$=0$
0	$+\mu_s(\xi^2+\beta^2)\cosh\alpha f$	$-\mu_s 2i\xi\beta \sinh\beta f$	$+\mu_s(\xi^2+\beta^2)\sinh\alpha f$	$-\mu_s 2i\xi\beta \cosh\beta f$	$-\lambda w(\eta^2-\xi^2)e^{-\eta f}$	$=0$
$-\lambda w(\eta^2-\xi^2)e^{-\eta f}$	$+\mu_s(\xi^2+\beta^2)\cosh\alpha f$	$+\mu_s 2i\xi\beta \sinh\beta f$	$-\mu_s(\xi^2+\beta^2)\sinh\alpha f$	$-\mu_s 2i\xi\beta \cosh\beta f$	0	$=0$
0	$+\mu_s 2i\xi\alpha \sinh\alpha f$	$+\mu_s(\xi^2+\beta^2)\cosh\beta f$	$+\mu_s 2i\xi\alpha \cosh\alpha f$	$+\mu_s(\xi^2+\beta^2)\sinh\beta f$	0	$=0$
0	$-\mu_s 2i\xi\alpha \sinh\alpha f$	$+\mu_s(\xi^2+\beta^2)\cosh\beta f$	$+\mu_s 2i\xi\alpha \cosh\alpha f$	$-\mu_s(\xi^2+\beta^2)\sinh\beta f$	0	$=0$

(19)

$$
\begin{vmatrix}
\eta e^{-\eta t} & \alpha \sinh \alpha f & -i\xi \sinh \beta f & 0 & 0 & 0 \\
-\frac{\lambda w}{\mu_s}(\eta^2-\xi^2)e^{-\eta t} & (\xi^2+\beta^2)\cosh \alpha f & -2i\xi\beta \cosh \beta f & 0 & 0 & 0 \\
0 & 2i\xi\alpha \sinh \alpha f & (\xi^2+\beta^2)\sinh \beta f & 0 & 0 & 0 \\
0 & 0 & 0 & \eta e^{-\eta t} & \alpha \cosh \alpha f & -i\xi \cosh \beta f \\
0 & 0 & 0 & -\frac{\lambda w}{\mu_s}(\eta^2-\xi^2)e^{-\eta t} & (\xi^2+\beta^2)\sinh \alpha f & -2i\xi\beta \sinh \beta f \\
0 & 0 & 0 & 0 & 2i\xi\alpha \cosh \alpha f & (\xi^2+\beta^2)\cosh \beta f
\end{vmatrix} = 0 \qquad (20)
$$

$$\varphi_0 = A_0 e^{+\eta y} e^{i(\omega t + \xi x)}$$
$$\varphi_1 = A_d \cosh \alpha y \, e^{i(\omega t + \xi x)}$$
$$\psi_1 = B_r \sinh \beta y \, e^{i(\omega t + \xi x)} \qquad (21)$$
$$\varphi_2 = A_2 e^{-\eta y} e^{i(\omega t + \xi x)}$$

provided $A_2 = + A_0$

24. These functions substituted into the boundary conditions give the upper diagonal minor of equation (20) as a condition for the existence of a solution. These four functions describe a motion of the plate symmetric about its median plane.

25. Alternatively, one can use

$$\varphi_0 = A_0 e^{+\eta y} e^{i(\omega t + \xi x)}$$
$$\varphi_1 = B_d \sinh \alpha y \, e^{i(\omega t + \xi x)}$$
$$\psi_1 = A_r \cosh \beta y \, e^{i(\omega t + \xi x)} \qquad (22)$$
$$\varphi_2 = A_2 e^{-\eta y} e^{i(\omega t + \xi x)}$$

provided $A_0 = -A_2$. These four functions can also satisfy all six boundary conditions, and lead to the lower diagonal minor of (20). They describe a motion of the plate antisymmetric about its median plane. In the case of wave lengths in x ($2\pi/\xi$) very much greater than the thickness of the plate, the symmetric and antisymmetric functions describe the so-called longitudinal and flexural vibrations of the plate, respectively.

26. One can therefore divide the discussion of the roots of the complete sixth-order determinant into separate discussions of the roots of the two third-order determinants. When any one amplitude A or B is given, the rest are determined by solving the set of five inhomogeneous equations obtained by dropping one of the six. Depending on whether the determinant for symmetric or antisymmetric motion has been set equal to zero, $A_0 = \pm A_2$, and either $B_d = A_r = 0$ or $A_d = B_r = 0$.

27. Before proceeding with the numerical evaluation of the roots of these determinants for given (ω), it would be well to point out some of the properties of these determinants, and their physical interpretation if any.

28. Either determinant defines an implicit relation between any two of the following variables: $\omega, \xi, c_p, \alpha, \beta, \eta$. c_p is the phase velocity in the x direction, defined as ω/ξ. For a fixed value (real or complex) of any one variable there is an infinite set of values for the other. As one varies continuously, the other defines an infinite family of functions.

29. Those values of ξ real, or nearly real, for given ω real, correspond to modes of vibration propagated along the plate with no or little attenuation. If a ξ_i has an appreciable imaginary component, this mode is highly damped. The energy associated with it may be said to leak off rapidly into the surrounding medium. In case a transient disturbance - or superposition of modes - is propagated along the plate, after a relatively short distance of travel only those modes with relatively small attenuation are significant in summing to describe the shape of the transient.

30. The determinants for symmetric and antisymmetric motion in equation (20) are closely related to Lamb's equations for determining the symmetric and antisymmetric modes of a plate in a vacuum. The minors in equation (20) can be written, using the definitions in equation (11):

Symmetric

$$[(\xi^2+\beta^2)^2 \cosh \alpha f \sinh \beta f - 4\xi^2 \alpha\beta \cosh \beta f \sinh \alpha f]$$

$$+ \left[\frac{\rho_w c_w^2}{\rho_s c_t^2} \frac{(\eta^2-\xi^2)}{\eta} \alpha(\beta^2-\xi^2) \sinh \alpha f \sinh \beta f\right] = 0 \qquad (23)$$

Antisymmetric

$$[(\xi^2+\beta^2)^2 \sinh \alpha f \cosh \beta f - 4\xi^2 \alpha\beta \sinh \beta f \cosh \alpha f]$$

$$+ \left[\frac{\rho_w c_w^2}{\rho_s c_t^2} \frac{(\eta^2-\xi^2)}{\eta} \alpha(\beta^2-\xi^2) \cosh \beta f \cosh \alpha f\right] = 0 \qquad (24)$$

31. If these equations are compared with the corresponding ones given by Lamb for a plate in a vacuum (Ref. 2, equations (12) and (48)), it will be seen that the first terms in equations (23) and (24) above are just his

equations (12) and (48). The second terms are corrections introduced by the water. If the density or velocity of sound in water in the second term is made to approach zero, the second term vanishes and equations (23) and (24) reduce to those derived by Lamb.

32. Now if the second term is small compared to the first, one can except that solutions to the complete equations (23) and (24) will be found close to those for the first term alone equals zero, i.e., close to the solutions already found by Lamb. The second term is small compared to the first, since $\rho_w c_w^2 / \rho_s c_r^2 \eta$ is small, except where $\eta \left(= \left(\xi^2 - \frac{\omega^2}{c_w^2}\right)^{1/2}\right)$.

is small. If the equations (23), (24) are multiplied by η, it will be seen that the smallness of η introduces additional solutions not in the neighborhood of those given by Lamb's solutions.

33. The equation for the symmetric case (23) is identical with the one for the antisymmetric case (24) except that hyperbolic sines in one replace hyperbolic cosines in the other, and vice versa. Therefore when the real parts of all the hyperbolic functions are large, the two expressions become practically identical. This is the case when the wavelength in x is small compared to the thickness of the plate, or when the problem approaches the case of a semi-infinite elastic solid. There is then no distinction between symmetric and antisymmetric motion.

34. There are solutions at $\beta = 0$ for all ω for the symmetric case, and at $\alpha = 0$ for all ω for the antisymmetric case. Physically, this corresponds to the fact that at any excitation frequency some sort of disturbance, though very small, must initially be propagated down the plate with velocity c_r or c_d.

35. For purposes of computation it will be useful to have equations (23) and (24) in dimensionless form. In terms of ξ, c_p they become:

Symmetric Case

$$4\left[\left(1 - \tfrac{1}{2}\frac{c_p^2}{c_r^2}\right)^2 \coth\left(\xi f\left(1 - \frac{c_p^2}{c_d^2}\right)^{1/2}\right) - \left(1 - \frac{c_p^2}{c_d^2}\right)^{1/2}\left(1 - \frac{c_p^2}{c_r^2}\right)^{1/2} \coth\left(\xi f\left(1 - \frac{c_p^2}{c_r^2}\right)^{1/2}\right)\right] +$$

$$+ \frac{\rho_w c_w^2}{\rho_s c_r^2} \frac{1}{\left(1 - \frac{c_p^2}{c_w^2}\right)^{1/2}} \frac{c_p^4}{c_w^2 c_r^2}\left(1 - \frac{c_p^2}{c_d^2}\right)^{1/2} = 0 \qquad (25)$$

Antisymmetric Case

$$4\left[\left(1-\frac{1}{2}\frac{c_p^2}{c_t^2}\right)^2 \tanh\left(\xi\zeta\left(1-\frac{c_p^2}{c_d^2}\right)^{1/2}\right) - \left(1-\frac{c_p^2}{c_t^2}\right)^{1/2}\left(1-\frac{c_p^2}{c_d^2}\right)^{1/2}\tanh\left(\xi\zeta\left(1-\frac{c_p^2}{c_t^2}\right)^{1/2}\right)\right] \quad (26)$$

$$+\frac{\rho_w c_w^2}{\rho_s c_t^2}\frac{1}{\left(1-\frac{c_p^2}{c_w^2}\right)^{1/2}}\frac{c_p^4}{c_w^2 c_t^2}\left(1-\frac{c_p^2}{c_d^2}\right)^{1/2} = 0$$

36. Evidently when $c_p \cong c_w$ both terms become of the same order of magnitude, so that there must be solutions for c_p in this neighborhood, almost independent of ω or ξ.

37. If for c_p one inserts $\frac{\omega}{\xi}$ in the above equations, and then holds ω fixed, it is evident that there must be solutions for ξ near $\xi = (2n+1)\pi i/h$ for the symmetric case, and near $\xi = n\pi i/h$ for the antisymmetric case. Both terms in equations (25) and (26) become small under these conditions for n sufficiently large. These are the higher modes, and evidently they are very highly attenuated since ξ is almost purely imaginary.

38. As previously stated, if ω is considered as a continuous variable, there are families of functions $\xi_i(\omega), c_{pi}(\omega)$ etc., defined by equations (25) and (26). Following Lamb, the lower and more important of these functions will be evaluated for ω as a purely real variable, in particular the principal phase velocity curves $c_{p_1}(\omega)$. Mathematically one finds where the contour of the real axis in the ω plane falls in the complex c_p plane, the mapping being defined implicitly by means of equations (23) and (24) or their equivalents (25) and (26). There are infinitely many Riemann surfaces, of which only the more important ones are selected. This information is needed in order to determine the behavior of a transient as it progresses along the plate.

V. EVALUATION OF THE PHASE VELOCITY FOR VERY LARGE AND VERY SMALL WAVELENGTHS

Branches Close to Lamb's Curves. Long Wavelength

39. For small values of ξ f (wavelength large compared to the thickness of the plate) the hyperbolic sines and cosines can be replaced by linear terms or unity. The phase velocity for the principal symmetric mode is in this case

$$c_p = c_r \sqrt{4\left(1 - \frac{c_r^2}{c_d^2}\right)} \left(1 + \frac{i}{2} \frac{\rho_w c_w^2}{\rho_s c_r^2} \frac{\omega t}{c_w} \left(\frac{1}{4\left(1 - \frac{c_r^2}{c_d^2}\right)} - \frac{c_r^2}{c_d^2}\right)\right) \qquad (27)$$

Lamb gives, under the same conditions for a plate in a vacuum (Ref. 1, equation (15)), just the above expression with $\rho_w = c_w = 0$. This is the velocity of "longitudinal" waves in an elastic plate.

40. Evidently the effect of the water on the propagation of long longitudinal waves is not to change the real part of the phase velocity at all, but to add a very small attenuation which, for low frequencies, increases as the frequency.

41. For long wavelengths, the determinant for the antisymmetrical modes gives for the phase velocity of long "flexural" waves,

$$c_p^2 = c_r^2 \left[\frac{4}{3} - \xi^3 \left(1 - \frac{c_r^2}{c_d^2}\right) \frac{\rho_s}{\rho_w}\right] \Big/ \left(1 + \xi + \frac{\rho_s}{\rho_w}\right) \qquad (28)$$

Here third order terms must be included in expanding the hyperbolic functions, since the entire determinant vanishes in the first and second order.

42. Lamb's expression for the same condition with a plate in a vacuum is (Ref. 2, equation (50)),

$$c_p^2 = c_r^2 \left[\frac{4}{3} + \xi^2 \left(1 - \frac{c_r^2}{c_d^2}\right)\right] \qquad (29)$$

which is the limit of (28) as $\rho_w \to 0$. Note however that with ξ or f very small and ρ_w finite, $c_p^2 \sim \xi^3 f^3$ for a plate in water, whereas $c_p^2 \sim f^2 \xi^2$ for a plate in a vacuum.

Consider this limiting form,

$$c_p^2 = \frac{4}{3} c_r^2 \left(1 - \frac{c_r^2}{c_d^2}\right) \frac{\rho_s}{\rho_w} \xi^3 f^3 \qquad (30)$$

and change to variables c_p and ω . Then,

Branch B_4

$$c_p = \left(\frac{4}{3} c_r^2 \left(1 - \frac{c_r^2}{c_d^2}\right) \frac{\rho_s}{\rho_w} f^3\right)^{1/5} \omega^{3/5} = \text{const}\ \omega^{3/5}$$

$$= \text{const}\ |\omega|^{3/5} e^{i0} \qquad (31)$$

Evidently if (31) satisfies (24) in the limit of ω small and pure real, with c_p real, then (24) is also satisfied by ω small and real with c_p complex. Equation (31) indicates that there are five different Riemann surfaces or branches from which a point of ω small and pure real in the ω plane can be mapped into the c_p plane. Of these five only equation (31) and

Branch B_2

$$c_p = \text{const}\ \left(|\omega| e^{4\pi i}\right)^{3/5}$$

$$= \text{const}\ |\omega|^{3/5} e^{i \frac{4}{5} \frac{\pi}{2}} \qquad (32)$$

are acceptable physically. The other three possible choices of angle for c_p, corresponding to $2\pi, 6\pi, 8\pi$ for the angle of ω , would indicate either propagation in the opposite direction, or negative attenuation.

43. There are therefore two acceptable phase velocities for long flexural waves represented in absolute magnitude by the same formula One is highly attenuated; the other is not attenuated at all.

Branches Close to Lamb's Curves. Short Wavelength.

44. The determinants for symmetric and antisymmetric motion approach the same limiting form for short wavelength, or ξ f large.

$$\left[(\xi^2+\beta^2)^2 - 4\xi^2 \alpha\beta\right] + \frac{\rho_w c_w^2}{\rho_s c_r^2} \frac{(\eta^2-\xi^2)}{\eta} \alpha(\beta^2-\xi^2) = 0 \qquad (33)$$

45. This is the same expression as that found by Lamb for a plate in a vacuum, again plus a small correction term due to the water. Lamb's

expression was the same as that deduced by Rayleigh for seismic waves on the surface of the earth. The above expression therefore corresponds to Rayleigh waves on the floor of the ocean.

46. The phase velocity can be deduced from (33) by assuming that $c_p = R(1+\epsilon)$, $\epsilon \ll 1$, where R is the velocity of Rayleigh waves, determined by setting the first term alone of equation (33) equal to zero. If $c_p = R(1+\epsilon)$ is substituted into equation (33), or the equivalent expressions (25) or (26) with the hyperbolic functions set equal to unity, one can evaluate ϵ. It is assumed that the second, water-correction term is small. In this way one finds

$$\text{Branches } B_1, B_2. \quad c_p = R(1+\epsilon) \tag{34}$$

where $$R = 0.9194\, c_r = 0.303 \cdot 10^6 \text{ cm/sec} \tag{35}$$

$$\epsilon = -i \frac{\left[\frac{\rho_w c_w^2}{\rho_s c_r^2} \cdot \frac{R^4}{c_w^2 c_r^2}\left(1-\frac{R^2}{c_d^2}\right)^{1/2}\right]}{4\sqrt{\frac{R^2}{c_w^2}-1}\left[2\frac{R^2}{c_r^2}\left(1-\frac{1}{2}\frac{R^2}{c_r^2}\right)-\frac{R^2}{c_d^2}\left(\frac{1-\frac{R^2}{c_r^2}}{1-\frac{R^2}{c_d^2}}\right)^{1/2}-\frac{R^2}{c_r^2}\left(\frac{1-\frac{R^2}{c_d^2}}{1-\frac{R^2}{c_r^2}}\right)^{1/2}\right]} \tag{36}$$

47. The numerical value for ϵ using the data in equation (11) is

$$\epsilon = i\ 1.18 \cdot 10^{-2} \tag{37}$$

Thus the attenuation of Rayleigh waves on a steel-bottomed ocean would be relatively small, so far as losses by acoustic radiation are concerned. In practice, since the wavelength of seismic waves is comparable to the depth of the ocean, the finite depth of the ocean and gravity waves on its surface would have to be taken into account.

Branches Not Close to Lamb's Curves.

48. The form of equations (25), (26), multiplied by $(1 - c_p^2/c_w^2)$, indicates that branches of the phase velocity curve may be found for c_p real and less than but almost equal to c_w. It can be shown that the first and

second terms of equations (25) and (26) are of opposite sign, so that they can be made to cancel. For c_p real, greater than but almost equal to c_w, the first term is imaginary and the second real; hence their sum can never vanish.

49. For ξf small, or long wavelengths, the determinant of the symmetric case may be approximated to give

Branch B_3

$$\frac{c_p}{c_w} = 1 - \frac{\left[\frac{\rho_w c_w^2}{\rho_s c_r^2}\left(1 - \frac{c_w^2}{c_d^2}\right)\frac{f\omega}{c_w}\right]^2}{32\left(1 - \frac{1}{4}\frac{c_w^2}{c_r^2} + \frac{c_r^2}{c_d^2}\right)}$$

$$= 1 - 1.25 \cdot 10^{-5}\left(\frac{f^2\omega^2}{c_w^2}\right)\left(\frac{f\omega}{c_w} < 1\right) \qquad (38)$$

50. For ξf small, c_p in the determinant for the antisymmetrical case does not remain close to c_w but approaches zero in one of the two ways indicated in equations (31) and (32). In fact, examination of the original equations (24) or (26) will show that as $\omega \to 0$, $\xi \to 0$ and always in such a way that $\frac{\omega}{\xi} = c_p \to 0$

51. For ξf large, or short wavelengths, the antisymmetric and symmetric forms approach each other, and if c_p is suspected to be real and less than c_w, the equation which must be satisfied is

$$\left(1 - \frac{c_p^2}{c_w^2}\right)^{1/2}\left[4\left(1 - \frac{1}{2}\frac{c_p^2}{c_r^2}\right)^2 - 4\left(1 - \frac{c_p^2}{c_d^2}\right)^{1/2}\left(1 - \frac{c_p^2}{c_r^2}\right)^{1/2}\right]$$

$$+ \frac{\rho_w c_p^2}{\rho_s c_r^2}\left(1 - \frac{c_p^2}{c_d^2}\right)^{1/2} = 0 \qquad (39)$$

52. These two terms are of opposite sign, so that $c_p < c_w$ and real is a possibility. Substituting $c_p = c_w$ in all terms except in the factor $\left(1 - \frac{c_p^2}{c_w^2}\right)^{1/2}$

one can obtain the approximate expression

Branches B_3, B_4.

$$\frac{c_p^2}{c_w^2} = 1 - \left\{ \frac{\frac{\rho_w c_w^4}{\rho_s c_r^4}\left(1 - \frac{c_w^2}{c_d^2}\right)^{1/2}}{4\left[\left(1 - \frac{c_w^2}{c_d^2}\right)^{1/2}\left(1 - \frac{c_w^2}{c_r^2}\right)^{1/2} - \left(1 - \frac{1}{2}\frac{c_w^2}{c_r^2}\right)^2\right]} \right\}^2 \qquad (40)$$

Using the numerical values in equation (11).

$$\frac{c_p}{c_w} = 1 - 0.000\ 19 \qquad (41)$$

53. In summary therefore, there is one symmetric and one antisymmetric branch of the phase-velocity curve close to c_w. They are both the same constant fraction of c_w at high frequencies, and real. At low frequencies the symmetric one approaches c_w quadratically with respect to frequency, and is real. The antisymmetric one must diverge from c_w and approach zero. It is also real, and was shown numerically to go into equation (31).

VI. EVALUATION OF THE PHASE VELOCITY FOR INTERMEDIATE WAVELENGTHS. CONNECTION OF THE BRANCHES.

54. Thus far the extremes only of the phase-velocity vs frequency curves have been evaluated, and compared with the results of Lamb for a plate in a vacuum. The various branches so found are summarized in Sketch 3, Lamb's curves, and Sketch 4, limiting curves for high and low frequency for a plate in water. A beaded line indicates that the phase velocity has a small imaginary component (slight attenuation), an open circle line indicates a large imaginary component (large attenuation), and a full line indicates that the phase velocity is all real (no attenuation). Full horizontal lines at c_d and c_r should appear on both sketches, but have been omitted to avoid confusion.

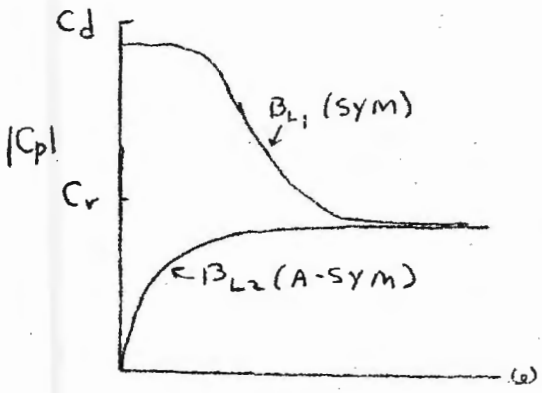

Sketch 3

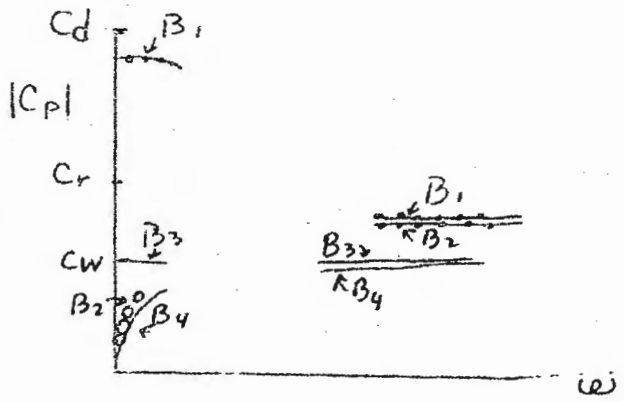

Sketch 4

55. Two questions now arise: where do the intermediate points on these branches lie and what branches on the left in Sketch 4 tie in with what branches on the right?

56. To answer these questions, consider the equations (24) and (25) as giving a functional relation between two complex variables implicitly. Choose for example c_p and ω. Either (24) or (25) can be written.

$$F(\omega, c_p) = R(c_{pr}, c_{pi}, \omega_r, \omega_i) + i\, I(c_{pr}, c_{pi}, \omega_r, \omega_i) = 0 \qquad (42)$$

where c_{pr}, c_{pi}, ω_r, ω_i are the real and imaginary parts of c_p and ω.

57. There are therefore three complex planes, the F plane, the c_p plane and the ω plane. Imagine that a point be fixed in the ω plane, and a point in the c_p plane describes a closed curve. The corresponding point in the F plane will also describe a closed curve, provided that $F(c_p, \omega)$ is regular over the range of variables considered. If the closed curve in the F plane incloses the origin, it means that a point on the implicit relation between c_p and ω, given by $F(c_p, \omega) = 0$ has been located. It lies somewhere within the closed curve in the c_p plane, for the given point ω.

58. This process was used to locate points in the intermediate regions of Sketch 4, to establish the connections between the right and left branches, and also as an independent numerical check on the analytic derivations of equations (27), (28), (36), (38) and (41). The procedure is as follows. A point ω_o, c_{po} is chosen either on one of Lamb's curves or in some other region where a solution is suspected, such as c_p close to c_w. The values $\omega_o, c_{po}(1+\epsilon e^{i\theta})$ are then substituted into equation (25) or (26), and each factor of each term expanded by Taylor's theorem. ϵ is assumed small compared to unity. In some cases, for example when c_p is near c_w,

ϵ must be very small indeed. If the choice ω_o, c_{po} was a good guess, the value of the determinant, equation (25) or (26), will become very small, and ϵ and θ can then be adjusted to ϵ_o, θ_o to make the entire expression vanish. When a value for ϵ_o has been so determined, one must subsequently check that the expansions used to obtain it were valid. A point on the implicit relation between ω and c_p, ω_o and $c_{p_o}(1+\epsilon_o e^{i\theta_o})$

has thus been determined.

59. In the case of Branch B_2, a method similar to that used to obtain equation (36) will give intermediate points on the phase-velocity curve. If one lets $F(\omega, c_p)$ stand for equation (25), the symmetric case, then

$$F(\omega, c_p) = \Delta_L(\omega, c_p) + c(\omega, c_p) = 0 \tag{43}$$

where Δ_L is Lamb's determinant for the plate in a vacuum and $c(\omega, c_p)$ is the small correction term due to the water. Let ω_o, c_{po}, be a point on Lamb's phase-velocity curve B_{L_1}, $(\Delta_L(\omega_o, c_{p_o}) = 0)$,

and substitute ω_o, $c_{po}(1+\epsilon)$ into equation (41).

$$F(\omega_o, c_{p_o}(1+\epsilon)) = \Delta_L(\omega_o, c_{p_o}) + \frac{\partial \Delta_L}{\partial c_{p_o}}(\omega_o, c_{p_o})\epsilon c_{p_o} + c(\omega_o, c_{p_o}) = 0$$

or

$$\epsilon = \frac{-c(\omega_o, c_{p_o})}{\frac{\partial \Delta_L}{\partial c_{p_o}} \cdot c_{p_o}} \tag{44}$$

Since $\frac{\partial \Delta_L}{\partial \omega}$ is easier to use than $\frac{\partial \Delta_L}{\partial c_p}$ one can also write

$$\epsilon = \frac{+\,c(\omega_o, c_{p_o})}{c_{p_o} \frac{\partial \Delta_L}{\partial \omega} \left(\frac{d\omega_o}{dc_{p_o}}\right)_{BL_1}} \tag{45}$$

where $(d\omega_0/dc_{p_0})_{B_{L1}}$ is taken graphically from Lamb's phase-velocity curve for B_{L1}, in Sketch 3 or Plate 1. Since for $c_{po} > c_w$ and real the correction term is pure imaginary, equation (45) leads to the conclusion that the water around the plate does not change the real part of the phase velocity, but only adds a small attenuation. Also, barring unusual behavior of $C(\omega_0, c_{p_0})$ and $\partial\Delta/\partial\omega$ this attenuation should be a maximum where $(d\omega_0/dc_{p_0})_{B_{L1}}$ is a minimum. This is at the intermediate frequencies, where the wavelength is neither large nor small compared to the thickness. This expectation was borne out by the numerical calculations (Plate 2).

60. If the process is applied to determining the antisymmetrical branch B_2, close to B_{L2}, it fails as $c_p \to c_w$, but in so doing indicates that the imaginary component of the phase velocity becomes very large. For this reason it was inferred that at low frequencies B_2 connected with the highly attenuated phase-velocity curve whose analytic expression is given in equation (32).

61. In this way the connections required for Sketch 4 were completed, and are indicated in Plate 1. Crosses (x) in Plates 1-5 indicate numerical values computed by one of the above methods. In Plate 1 the absolute magnitudes of all the phase velocities are plotted as a function of the circular frequency ω. The separation of B_1 and B_{L1}, B_2 and B_{L2} is somewhat exaggerated. In Plates 2-5 the detailed dependence of the individual branches on the dimensionless variable $\omega f/c_w$ is given, so that these curves can be applied to a plate of any thickness. The solid lines indicate analytic curves, and the dotted lines the interpolated guess. For branches B_1 and B_2, (Plates 2 and 3) the imaginary component of the phase velocity c_p is plotted against the real component, with $\omega f/c_w$ as parameter for the check points. For branches B_3 and B_4, (Plates 4 and 5) which are all real and close to c_w, $1 - c_p/c_w$ was used as dependent variable, and $\omega f/c_w$ as independent variable.

62. In Plate 1 the symmetric branch B_1 followed quite closely the corresponding Lamb curve B_{L1} throughout. The imaginary component has a maximum at intermediate values of wavelength ($\omega f/c \sim b$, Plate 2). The irregularity of the points for large and small $\omega f/cw$ reflects the difficulty of following the curve numerically in these regions.

63. In Plate 1 the antisymmetric branch B_2 clings closely to the Lamb branch B_{L2} until it dips to the c_w level. It then diverges rapidly from the Lamb curve in that its imaginary component becomes very large. At low frequencies it has the same absolute magnitude dependence on ω as branch B_4, and is close to B_{L2} in absolute magnitude, but the imaginary component is large (Plate 3).

64. Physically, we may interpret this antisymmetric mode as a high-pass filter, the cutoff point being determined approximately at that frequency where the phase velocity equals the velocity in the surrounding medium, water. Frequencies below this cutoff, where $c_p < c_w$, are highly attenuated, the energy being lost by radiation into the water. Above it, where $c_p > c_w$, they are only slightly attenuated.

65. In Plates 1 and 4, the symmetric branch B_3 is close to the velocity of sound in water throughout. At high frequencies it merges into B_4 at a constant fraction of c_w; at low frequencies it approaches c_w.

66. In Plates 1 and 5, the antisymmetric branch B_4, also just below c_w at high frequencies, follows the c_w level closely, almost to the point where it would cross the Lamb antisymmetric branch B_{L2} (Plate1). It then turns abruptly down, and remains just below the Lamb branch B_{L2}. It is real throughout. It is very difficult to explore numerically the antisymmetric case for small ω, since all the terms are approaching zero. In this region it was necessary to carry out the analysis with the variables c_p and ξ, and subsequently to convert to c_p and ω.

67. The dimensionless variable $\omega f/c_w$ used in Plates 2-5 is the ratio of the time required for sound to traverse the half thickness of the plate in water to the time required for the exponent in the time-dependent factor $e^{i\omega\tau}$ in φ or ψ to change through one radian. It will be observed that, except for branch B_1, when this ratio is of order unity most of the changes in the phase velocity curves are taking place. Branch B_3 is beginning to approach c_w (Plate 4), B_4 is turning sharply down (Plate 1), and B_2 is changing from predominantly real to predominantly imaginary (Plate 3). The frequency corresponding to $\omega f/c_w \sim 1$ is 160 kc, period ~ 6 μsec. For Branch B_1 the change occurs around $\omega f/c_w \sim 5$, or at a frequency of approximately 800 kc, period ~ 1.2 μsec. A conversion scale from $\omega f/c_w$ to ω appears on Plate 1.

VII. USE OF PHASE VELOCITY CURVES IN THE STUDY OF TRANSIENTS

68. According to Lamb (Ref. 4), in a one-dimensional dispersive medium the effect of an initial disturbance can be represented by an integral of the form

$$\varphi(x,t) = \int_0^\infty A(\xi)\, e^{i(\omega\tau \pm \xi x)}\, d\xi \qquad (46)$$

where ω as a function of ξ is determined by the phase-velocity curve, which in this report is given as $c_p = \omega/\xi$ as a function of ω. $A(\xi)$ is the Fourier

transform of the shape of the disturbance at t=0. For example, if $A(\xi) =$ constant, the initial disturbance is infinitely concentrated, a δ function. If $A(\xi) = \pi\delta(\xi) - i/\xi$ the initial disturbance is a step, or unit function, $1(x)$.

69. For the problem of the elastic plate in water, equation (46) would be generalized to

$$\varphi_0 = \sum_{i=1}^{\infty} \int_0^{\infty} A_{0i}(\xi) e^{+\eta_i y} e^{i(\omega_i t + \xi x)} d\xi$$

$$\varphi_1 = \sum_{i=1}^{\infty} \left[\int_0^{\infty} \left(A_{1i}(\xi) \cosh \alpha_i y e^{i(\omega_i t + \xi x)} + B_{1i}(\xi) \sinh \alpha_i y e^{i(\omega_i t + \xi x)} \right) d\xi \right]$$

$$\psi_1 = \sum_{i=1}^{\infty} \left[\int_0^{\infty} \left(A_{1i}(\xi) \cosh \beta_i y e^{i(\omega_i t + \xi x)} + B_{1i}(\xi) \sinh \beta_i y e^{i(\omega_i t + \xi x)} \right) d\xi \right] \quad (47)$$

$$\varphi_2 = \sum_{i=1}^{\infty} \int_0^{\infty} A_{2i}(\xi) e^{-\eta_i y} e^{i(\omega_i t + \xi x)} d\xi$$

In (47), $\omega_i, \alpha_i, \beta_i, \eta_i$ are functions of ξ determined by the phase-velocity curves, and the summation is applied over all the branches - an infinite number of them, i.e. all the normal modes. The $A_{1i}(\xi)$ and $B_{1i}(\xi)$ are so chosen that the configuration of the φ_1 and ψ_1 with respect to y and x is correctly given at the initial instant, $t = 0$.

70. However the amplitudes $A_{1i}(\xi)$, $B_{1i}(\xi)$ of the higher modes are appreciable only when there is considerable "structure" or variation with respect to y in the initial disturbance, not true in the present problem. Also it was shown that these higher modes are damped out rapidly as the disturbance progresses across the plate. Therefore it will be considered sufficient to use only the lowest members, or branches of the phase-velocity curve which have just been determined.

71. Even if the amplitudes $A_{1i}(\xi)$, $B_{1i}(\xi)$ could be determined there would still remain the difficult problem of carrying out the integration over ξ, where the relations $\omega_i(\xi)$ and $\alpha_i(\xi)$ etc. are defined implicitly and the variables are actually complex. The problem of contour integration of a function of a complex variable defined implicitly seems to have no known general solution. Here the path of integration is along the real axis, but it could be deformed. Lamb (Ref. 4) gives an approximate method which will be modified slightly to apply to the present problem.

72. The oscillograms in Plate 8, showing the precursor, represent observations of pressure as functions of t , for various values of x, with y fixed, as shown in Sketch 1. Therefore the problem is to evaluate, say from φ_{2_3}

$$\left(p_{xx}\right)_{\rho_1} = \left(p_{yy}\right)_{\rho_2} = \lambda_w\left(\frac{\partial^2\varphi_2}{\partial x_2} + \frac{\partial^2\varphi_2}{\partial y_2^2}\right) = \lambda_w \sum_i \int_0^\infty (\eta_i^2 - \xi^2) A_{2i}(\xi)\, e^{-\eta_i y} e^{i(\omega_i \tau + \xi x)}\, d\xi \qquad (48)$$

as a function of t, with x as parameter. One would like to know what characteristic frequency or frequencies appear, i.e., the average "spacing of the crests" (Ref. 4) which appear in the oscillogram. Assume that the factor $(\eta_1^2 - \xi_1^2) \cdot A_{2i}\,\xi$ changes slowly by comparison to the factor $e^{i(\omega\tau + \xi x)}$. This will be true for a concentrated δ or step disturbance, and will also be true for an exponential-type explosion wave. Then the principal contribution to the integrand comes in those ranges of ξ where the exponent is stationary, since then all the elemental vectors represented by the integrand add in a straight line. The ω corresponding to this ξ is the one which appears predominantly in the oscillogram and determines the average spacing of the crests. The wavelength $2\pi/\xi$ would characterize a "snapshot" or instantaneous picture of the disturbance. The factor $e^{-\eta y}$ is neglected, since y is a constant. Hence this factor does not affect the relative value, with respect to x and t, of the integral.

73. To determine this characteristic ω, a modification of the construction given by Lamb (Ref. 4), is used. In Sketch 5

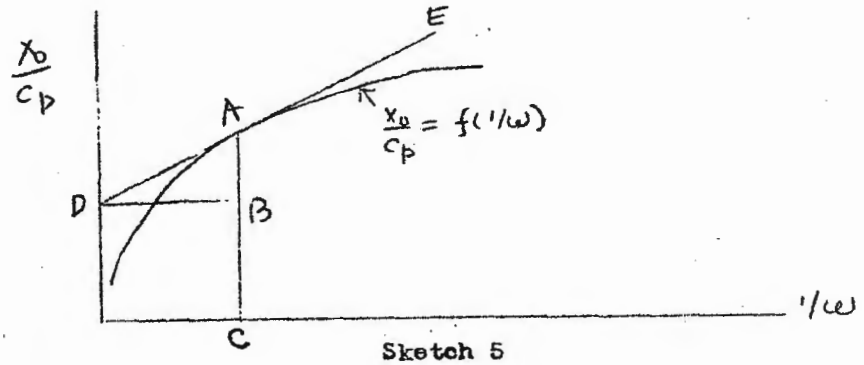

Sketch 5

x_0/c_p is plotted against $1/\omega$, where x_0 is the x coordinate of the point of observation. The ordinate has therefore the dimension of time. At any particular time t', given by a point on the y axis, the characteristic oscillation frequencies are given by the abscissae of the points of tangency, such as C, of straight lines drawn from the point t' to the x_0/c_p curve. Let A be in the first instance any point, not necessarily the tangent, on the x_0/c_p curve. The angle ADB has as tangent AB/BD, which is

$$\left(\frac{x_0}{c_p} - t'\right)\Big/(1/\omega) = \omega\left(\frac{x_0}{c_p} - t\right) = \xi x_0 - \omega t' \qquad (49)$$

and this tangent; hence the phase angle $\xi x - \omega t$ is stationary when the line DE is drawn tangent to the x_0/c_p curve. Evidently, as time goes on, the point D moves up the y axis, and the tangent line rolls on the x_0/c_p curve. If this curve is concave down, as drawn, $1/\omega$ increases and the maxima in the oscillogram become farther and farther apart. The characteristic frequency decreases with time. When the x_0/c_p curve is concave up, the opposite is true. If the x_0/c_p curve has sharp bends in it, as time goes on and and D moves up, the abscissa C of the characteristic frequency shifts only slightly. Thus over a considerable interval of time the spacing of the crests remains nearly the same, and this particular oscillation will appear very prominently in the oscillogram. In general in a dispersive medium, when the phase velocity vs frequency curve changes rapidly, i.e. has bends, the frequency characteristic of the transition region will appear in a transient disturbance. The commonest example of this is given by electrical filters with sharp cutoffs (c_p becomes almost all imaginary) or abrupt changes in their transmission characteristics. When excited by a transient, these filters often "ring" with oscillations characteristic of the cutoff or transition regions.

74. For a bend in the x_0/c_p curve to be sharp enough to make the corresponding frequency in the oscillogram prominent, a shift of $\Delta t'$ at D, Sketch 5, equal to the period corresponding to C, P_C, must cause a shift in P_C small compared to P_C. In other words the bend must be so sharp that the characteristic period changes by a small fraction of itself over the period of a single oscillation.

$$\frac{dP_c}{dt} << 1 \qquad (50)$$

75. If there is no dispersion in the medium, as in open water, the x_0/c_p curve is a straight line parallel to the $1/\omega$ axis. Then no tangent can be drawn until $t' = x_0/c_p$, when tangent and x_0/c_p curve coincide, or are tangent at all values of $1/\omega$. That is, the original undistorted disturbance, or at least an aperiodic disturbance, is observed.

76. The method of stationary phase described above, applies primarily to cases where ω and ξ are all real. For complex values, the saddle point method can be applied, which amounts to deforming the path of integration

from the real axis (stationary phase method) into the complex plane. However, when the relation between ω and ξ is defined implicitly, this process usually becomes too complicated to be tractable, though a formal solution can be written down. In the present problem the stationary phase method will be used, using only the real part of c_p, and the imaginary part(or the attenuation) will be neglected. This is probably a good approximation for all the branches except the low-frequency end of B_2, since everywhere else the imaginary part of c_p is exceedingly small. This approximation is equivalent to assuming that all the elemental vectors $e^{i(\omega t+\xi x)}$ are of the same length. When the tangent falls on that part of B_2 with large attenuation, where the approximation is known to fail, the entire contribution from that branch will be neglected, on the grounds that those frequencies will be damped out.

77. This approximation is a mathematical necessity, for which the justification is perhaps a little meagre. As it turns out, the precursor can be associated with Branch B_4, which is all real, so that where the theory agrees with observation, the approximation is valid.

VIII. APPLICATION OF STATIONARY PHASE METHOD

78. These arguments can be applied to the present problem of the propagation of the explosion wave along a steel plate in water. In Plates 6 and 7 is plotted $1/c_p$ vs $1/\omega$ for all the phase-velocity curves evaluated. $1/c_p$ was chosen rather than x_o/c_p with a particular x_o, since the shape of the curves would be unaffected by including x_o. The origin in coordinates x and t is the edge of the plate at the time the explosion wave strikes it. A point in time on the $1/c_p$ axis in Plate 6 (such as C) is at such a distance from the origin that a disturbance traveling with the velocity c_r would have just reached it. A disturbance traveling with a velocity c_d would have already gone by. It would have arrived at an earlier (smaller) time corresponding to the point A. Plate 6 can, by a proper choice of scale for the $1/c_p$ axis, therefore be made to apply to any position of the gauge.

79. Consider for example the observed oscillograms when the gauge is at the middle of the disc, 30.5 cm from the edge. The explosion lies nearly in the plane of the disc, so that the explosion wave strikes the disc on its edge, as in Sketch 6, paragraph 90.

80. At t=0, the origin (Plate 6), no tangents can be drawn and there is no disturbance at the gauge. At time $t=x/c_d$ (A, Plate 6), corresponding to the time required for a wave in the plate to reach the position of the gauge, traveling with a velocity c_d, a tangent to the straight line solution $1/c_p=1/c_d$ can be drawn. This is tangent at all frequencies. It does not

necessarily follow that the resulting disturbance will be similar to the original disturbance, but merely that it will be aperiodic (Ref. 5).

81. Shortly after $t=x/c_d$ another aperiodic disturbance will arrive corresponding to the tangent to the low frequency end of B_1 (Point B), or long longitudinal waves. Later two more aperiodic disturbances arrive (Points C, D), corresponding to the arrival of "underwater Rayleigh waves" on the surface of the plate and the straight line solution $1/c_p = 1/c_r$.

82. At intermediate and immediately subsequent times (Points B_1, D_1) tangents to the knees of branch B_1 can be drawn, with characteristic oscillations ranging in period between 0.6 to 1.9 μsec, or $1/\omega$ from 0.1 to 0.3 μsec. These are too short to be easily observed on the oscillograph with the sweep speed actually used.

83. Beginning at a time corresponding approximately to D_2, tangents can be drawn to Branch B_4. Since B_4 is concave up, as time goes on the tangent rolls toward the $1/c_p$ axis and the spacing of the crests in the oscillogram decreases until at $t = x/c_w$ (Point E) another aperiodic disturbance which has been traveling with a velocity equal to the velocity of sound in water arrives. This is just the behavior of the precursor, which precedes the main explosion wave in the water. Much later, at a time such as E_1 (see also Plate 7), tangents which fulfill the condition for periodicity can be drawn to the parabolic, concave-down part of branch B_4. This characteristic oscillation has a decreasing frequency, or increasing spacing of the crests.

84. The procedure outlined above does not give any indication of the treatment accorded Branch B_2, which shifts rapidly from primarily real to primarily imaginary at about $1/\omega=1.2$ μsec. If the analogy of B_2 to a high-pass filter is good, it might be suspected that oscillations characteristic of the cutoff frequency should appear, when this mode is sufficiently excited by the transient. The tangent which can be drawn to the primarily real part of B_2, between times C and D, does not fulfill the condition for periodicity.

85. The observations (Plate 8) made with a tourmaline pressure gauge and a cathode-ray oscillograph, can be compared with the above description of the periodic and aperiodic disturbances arriving at the center of the disc. There are a number of discrepancies. None of the disturbances corresponding to $1/c_d$, $1/c_r$, and branch B_1 appear. The absence of pulses corresponding to $1/c_d$ and $1/c_r$ must be attributed to smallness of the corresponding amplitude factors, $A_{c_d}(\xi)$ and $A_{c_r}(\xi)$.

The theory is insufficient to determine these factors, but from a physical standpoint one would expect them to be small. They represent disturbances propagated in the plate as though it were an infinite medium. Actually it is quite thin in terms of wavelengths to which the measuring instrument is responsive. Other investigations of more favorable examples have shown that these amplitudes are relatively small (Ref. 5).

86. The tangent points to the knees and the Rayleigh region end of B_1 fall at abscissae of high frequency, $\gtrsim$ one megacycle, which the oscillograms cannot resolve. The absence of a disturbance corresponding to the low-frequency part of B_1 remains unexplained, unless one wishes to infer from the observations that the amplitude factor here is small. For very low frequencies the wavelength is comparable to the radius of the disc, and the theory is not applicable.

87. The same remarks also apply to branch B_2. Here the low-frequency end is highly attenuated. It may be that the cutoff frequency is contributing to the precursor.

88. The lower tangent to B_4 gives a very satisfactory explanation of the precursor. Theory and observation of the velocity, the duration, the number of oscillations, and their range of period can be compared in the following table.

	Theory	Observed (from Report II)
Velocity	0.19×10^6 cm/sec	0.21×10^6 cm/sec
Duration	40 μsec	40-70 μ sec
Range of period	12 to 6 μsec	11 to 8.5 μsec
Number of oscillations	5	6

In Plate 6, if D_2 is specified at 52 μsec/cm, the velocity of the precursor corresponds to D_2, the duration to $x/c_{D2} = x/c_w$, with x = 1 ft. (30.5 cm). The range in period of the characteristic oscillation corresponds to $1/\omega$ = 2 μsec to $1/\omega$ = 1 μsec.

89. Also note that the duration of the precursor (and hence the number of oscillations) increases linearly with the scale of the y axis, or distance from the edge of the plate. This is in agreement with observation. The theory is insufficient to describe either the amplitude of the precursor as a function of time or the large negative peak often observed just

before the main shock wave. A good example of this negative peak appears in Plate 8, No. 6.

90. The above analysis applies to the case where the explosion wave lies nearly in the plane of the disc, at angles of incidence near 90°, as in Sketch 6. Evidently if the explosion wave comes from a direction more nearly normal to the disc, as in Sketch 7, it will arrive sooner at the gauge. Hence it will overlap the precursor, and precursor oscillations will appear after the arrival of the shock front. At an angle of incidence of about arc-cos $(c_w/c_{prec.}) \doteq 57°$, precursor and explosion wave will arrive simultaneously, i.e., there is no "pre"cursor. This conclusion is also in approximate agreement with observation.

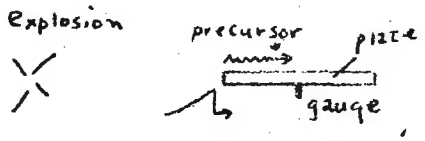

Sketch 6.

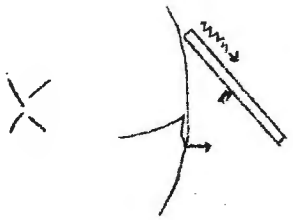

Sketch 7.

91. Theory requires that there should also be oscillations of period increasing with the time, corresponding to an upper tangent on the parabolic part of B_4, in Plate 7. These oscillations are those given by the classical theory of a struck bar, or flat plate (Ref. 6). The periodicity condition begins to be fulfilled at about point E_1 (Plates 6, 7) or about 150 μsec after the beginning of the precursor. The time scale on Plate 7 refers to the center of the disc, for $x_o \doteq 1$ ft $\doteq$ 30.5 cm. The period of oscillation should be initially about 75 μsec, corresponding to $1/\omega \doteq 12$ μsec.

92. These oscillations were not observed for any orientation of the disc. Near normal incidence, as in Plate 8, No. 2, an oscillation with qualitatively the correct properties, but with too short a period (14-30 μsec) was observed, just at the end of the oscillogram. This "postcursor" is unexplained; it may be quite unrelated to Branch B_4.

93. The fact that the observations fail to show these flexural vibrations should not be considered a serious objection to the theory. Their wavelength in the plate is comparable ~~to the theory. Their wavelength in the plate is comparable~~ to the radius of the disc, so that here the semi-infinite plate theory is no longer applicable.

94. Generally speaking, the theory developed for the semi-infinite plate can be expected to fail for times appreciably after the shock front, and for long-wavelength phenomena. For such cases the finite radius of the disc must be taken into account.

IX. SUMMARY AND CONCLUSIONS

95. The problem of the action of an underwater explosion wave on a water-backed elastic plate can be divided into two parts. In the first the plate is considered as in infinite slab, with the explosion wave as an incident plane wave transient. In the second the plate is considered as a wave guide, with the explosion wave setting the initial conditions at the edge of the plate. The first is an inhomogeneous boundary value problem, the second a homogeneous one.

96. The inhomogeneous case has been solved in the literature (Ref. 3), and the results of the theory are in qualitative agreement with the experiments on transients. The homogeneous problem forms the principal part of this report.

97. The phase-velocity curves as functions of frequency, for the principal normal modes of a plate in water, are closely related to the corresponding curves for a plate in a vacuum. The effect of the water on the principal symmetric mode of the plate is not to change the real part of the phase velocity from its value for a plate in a vacuum, but to add a small imaginary component, or attenuation due to radiation loss into the water. The principal antisymmetric mode is slightly attenuated at high frequencies, and strongly attenuated at low frequencies. The cutoff comes at that frequency where the phase velocity along the plate equals the velocity of sound in water.

98. In addition to the above two modes, which correspond to the principal modes for a plate in a vacuum, the presence of the water introduces two additional modes, one symmetric and one antisymmetric. At high frequencies their phase velocities are very close to, but a constant fraction of, the velocity of sound in water. At low frequencies the phase velocity of the symmetric mode approaches the velocity of sound in water; the phase velocity of the antisymmetric mode approaches zero. Both these modes are unattenuated, i.e. their phase velocities are all real. The antisymmetric mode accounts for most of the properties of the precursor, an oscillation which precedes the explosion wave as it travels along the plate.

REFERENCES

1. Love, The Mathematical Theory of Elasticity, IV ed., p. 309, Cambridge University Press, 1927.

2. Lamb, H., Proc. Roy. Soc. Lon. A, Vol. 93, p. 114 (1917).

3. Reissner, H., Helv. Phys. Acta, Vol. 2, p. 140, (1938).

4. Lamb, H., Hydrodynamics, IV ed., p. 396, Cambridge University Press, 1932.

5. Lamb, H., Phil. Trans. Roy. Soc. Lon. Series A, Vol. 203, p. 1 (1904).

6. Rayleigh, Lord., Theory of Sound, Vol. 1, p. 302, MacMillan & Co., London, 1894 (reprinted 1929).